inorganics

MDPI

Article

Functionalized Tris(anilido)triazacyclononanes as Hexadentate Ligands for the Encapsulation of U(III), U(IV) and La(III) Cations

Alasdair Formanuik [1], Fabrizio Ortu [1,2], Iñigo J. Vitorica-Yrezabal [1], Floriana Tuna [1], Eric J. L. McInnes [1], Louise S. Natrajan [1,*] and David P. Mills [1,*]

[1] Department of Chemistry, The University of Manchester, Oxford Road, Manchester M13 9PL, UK; aformanuik@outlook.com (A.F.); fabrizio.ortu@leicester.ac.uk (F.O.); inigo.vitorica@manchester.ac.uk (I.J.V.-Y.); floriana.tuna@manchester.ac.uk (F.T.); eric.mcinnes@manchester.ac.uk (E.J.L.M.)

[2] School of Chemistry, University of Leicester, University Road, Leicester LE1 7RH, UK

* Correspondence: louise.natrajan@manchester.ac.uk (L.S.N.); david.mills@manchester.ac.uk (D.P.M.); Tel.: +44-161-275-1426 (L.S.N.); +44-161-275-4606 (D.P.M.)

Abstract: Tripodal multidentate ligands have become increasingly popular in f-element chemistry for stabilizing unusual bonding motifs and supporting small molecule activation processes. The steric and electronic effects of ligand donor atom substituents have proved crucial in both of these applications. In this study we functionalized the previously reported tris-anilide ligand {tacn(SiMe$_2$NPh)$_3$} (tacn = 1,3,7-triazacyclononane) to incorporate substituted aromatic rings, with the aim of modifying f-element complex solubility and ligand steric effects. We report the synthesis of two proligands, {tacn(SiMe$_2$NHAr)$_3$} (Ar = C$_6$H$_3$Me$_2$-3,5 or C$_6$H$_4$Me-4), and their respective group 1 transfer agents—{tacn(SiMe$_2$NKAr)$_3$}, M(III) complexes [M{tacn(SiMe$_2$NAr)$_3$}] for M = La and U, and U(IV) complexes [M{tacn(SiMe$_2$NAr)$_3$}(Cl)]. These compounds were characterized by multinuclear NMR and FTIR spectroscopy and elemental analysis. The paramagnetic uranium complexes were also characterized by solid state magnetic measurements and UV/Vis/NIR spectroscopy. U(III) complexes were additionally studied by EPR spectroscopy. The solid state structures of all f-block complexes were authenticated by single-crystal X-ray diffraction (XRD), together with a minor byproduct [U{tacn(SiMe$_2$NC$_6$H$_4$Me-4)$_3$}(I)]. Comparisons of the characterization data of our f-element complexes with similar literature examples containing the {tacn(SiMe$_2$NPh)$_3$} ligand set showed minor changes in physicochemical properties resulting from the different aromatic ring substitution patterns we investigated.

Keywords: f-element; lanthanide; actinide; multidentate ligand; macrocycle

Citation: Formanuik, A.; Ortu, F.; Vitorica-Yrezabal, I.J.; Tuna, F.; McInnes, E.J.L.; Natrajan, L.S.; Mills, D.P. Functionalized Tris(anilido)triazacyclononanes as Hexadentate Ligands for the Encapsulation of U(III), U(IV) and La(III) Cations. *Inorganics* **2021**, *9*, 86. https://doi.org/10.3390/inorganics9120086

Academic Editor: Duncan H. Gregory

Received: 21 October 2021
Accepted: 24 November 2021
Published: 28 November 2021

1. Introduction

Coordinatively unsaturated metal complexes with well-defined reactive sites are ideal candidates for systematic reactivity studies, and as with the rest of the periodic table, such systems can be accessed for f-elements through the use of judiciously selected ligands [1]. Given the predominantly electrostatic bonding regimes and large ionic radii of f-elements, sterically demanding ligands with hard donor atoms provide the kinetic and electronic stabilization required to give robust complexes [2]. Multidentate and macrocyclic ligands form a privileged subset over their monodentate analogues in f-element coordination chemistry, as they can impart additional thermodynamic stability [1,2]. Tripodal examples, which exhibit approximate C_3 symmetry in solution, have proved particularly effective in controlling the coordination sphere of uranium by encapsulating the metal ion in a single well-defined "steric pocket" along the C_3 axis. Such motifs have supported unusual uranium oxidation states and bonding regimes, and coordinatively unsaturated U(III) centers that support rich small molecule activation chemistry [3–7].

Over the last 25 years, the tripodal ligands that have proved most popular for generating landmark uranium complexes include the anchored tris-aryloxides {$N(CH_2OAr)_3$} (Ar = substituted aryl), {$tacn(CH_2OAr)_3$} (tacn = 1,3,7-triazacyclononane) and {$Mes(CH_2OAr)_3$} (Mes = $C_6H_2Me_3$-2,4,6); and the tris-amides {$N(CH_2CH_2NSiR_3)_3$} (SiR_3 = $SiMe_3$, Si^tBuMe_2, Si^iPr_3) [3–7]. Several related macrocyclic ligand systems have more recently been applied in f-element chemistry [8–10]. f-Element complexes of tripodal ligands that impose approximate C_3 symmetry have been applied in the electrocatalytic reduction of water [11–13], and it has been shown that the steric and electronic effects of substituents on donor atoms of these ligands are crucial for dictating the physicochemical properties of resultant complexes. For example, the reaction of CO_2 with [U{$tacn(CH_2Ar^{tBu,tBu}O)_3$}] ($Ar^{tBu,tBu}O$ = 3,5-di-*tert*-butyl-2-oxybenzyl) gives the dinuclear U(IV) bridging oxo complex [{U[$tacn(CH_2Ar^{tBu,tBu}O)_3$]}$_2$(μ-O)] [14], whereas the more sterically demanding [U{tacn ($CH_2Ar^{Ad,Ad}O)_3$}] ($Ar^{Ad,Ad}O$ = 3-adamantyl-5-*tert*-butyl-2-oxybenzyl) reacts with CO_2 to yield the remarkable terminal CO_2 U(IV) complex [U{$tacn(Ar^{Ad,Ad}O)_3$}(CO_2)] [15]. Those examples showcase how the outcomes of small molecule activation reactions for tripodal U(III) complexes are dependent upon the size of the axial reactivity pocket [3–7].

By contrast, there have only been a handful of reports to date of the synthesis and physicochemical properties of uranium complexes of the related tris-anilido ligand {$tacn(SiMe_2NPh)_3$} [16–20]. However, it has already been shown that the $SiMe_2$ linkers engender considerable flexibility compared to the more rigid substituted aryl groups in [U{$tacn(CH_2ArO)_3$}] [3–7]. For example, the nearly trigonal prismatic arrangement of *N*-donor atoms in the U(III) complex [U{$tacn(SiMe_2NPh)_3$}] [16] is lost upon oxidation by elemental sulfur to give the distorted bicapped trigonal bipyramidal dinuclear U(IV) complex [{U[$tacn(SiMe_2NPh)_3$]}$_2$(μ-S)] [17], whilst approximate C_3 symmetry is typically retained when the U(III) complexes [U{$tacn(CH_2ArO)_3$}] are converted to U(IV/V/VI) products [3–7].

Herein we report the synthesis of two novel tris-anilido ligands with substituted aryl rings, {$tacn(SiMe_2Nar)_3$} (Ar = $C_6H_3Me_2$-3,5; C_6H_4Me-4). We utilized group 1 transfer agents of these ligands to synthesize U(III), La(III) and U(IV) complexes; and we characterized these complexes by a variety of techniques in order to compare these data with respective literature examples of lanthanum and uranium complexes of the unsubstituted ligand {$tacn(SiMe_2NPh)_3$}.

2. Results

2.1. Synthesis

The ligand precursors {$tacn(SiMe_2NHAr)_3$} (Ar = C_6H_4Me-4, **1-H$_3$**; $C_6H_3Me_2$-3,5, **2-H$_3$)** were prepared by modifications of the reported synthesis of {$tacn(SiMe_2NHPh)_3$} [21] (Scheme 1). The substituted anilines $NH_2C_6H_4Me$-4 and $NH_2C_6H_3Me_2$-3,5 were separately reacted with excess NaH in THF to provide the sodium anilides $NaNHC_6H_4Me$-4 and $NaNHC_6H_3Me_2$-3,5. These salts were filtered from the remaining NaH and were separately added dropwise to toluene solutions of {$tacn(SiMe_2Cl)_3$} [21] to give **1-H$_3$** and **2-H$_3$**, respectively, as pale yellow oils in very good yields after removal of volatiles under reduced pressure. The proligands were both reacted with excess KH in THF without further purification to afford the group 1 transfer agents {$tacn(SiMe_2NKC_6H_4Me\text{-}4)_3$}·2THF (**1-K$_3$**) and {$tacn(SiMe_2NKC_6H_3Me_2\text{-}3,5)_3$}·THF (**2-K$_3$**), respectively, in fair–good yields as off-white powders (Scheme 1). Despite repeated attempts, crystals of **1-K$_3$** and **2-K$_3$** suitable for analysis by single-crystal X-ray diffraction could not be obtained, but elemental analysis values obtained from powders dried in vacuo for 1 h indicated that bound THF molecules remained, as is the case for the Li and Na salts of {$tacn(SiMe_2NPh)_3$} [21].

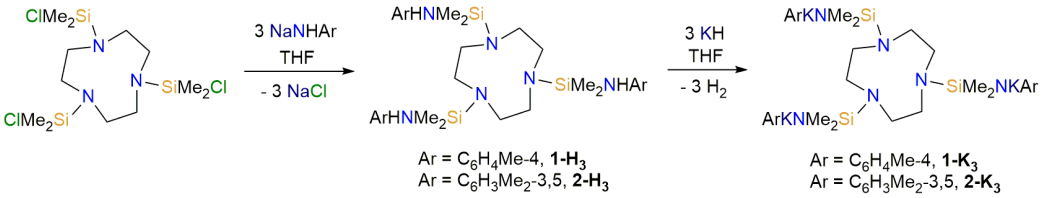

Scheme 1. Synthesis of proligands **1-H$_3$** and **2-H$_3$**, and the group 1 transfer agents **1-K$_3$** and **2-K$_3$**.

With **1-K$_3$** and **2-K$_3$** in hand, we adapted the syntheses of [La{tacn(SiMe$_2$NPh)$_3$}(THF)] and [U{tacn(SiMe$_2$NPh)$_3$}] [16] to perform separate salt metathesis reactions with [La(I)$_3$(THF)$_4$] [22] and [U(I)$_3$(THF)$_4$] [23] in THF to give [M{tacn(SiMe$_2$NC$_6$H$_4$Me-4)$_3$}] (M = La, **3-La**, U, **3-U**) and [M{tacn(SiMe$_2$NC$_6$H$_3$Me$_2$-3,5)$_3$}] (M = La, **4-La**, U, **4-U**) in fair yields following work-up and recrystallization (Scheme 2). We first performed the lanthanum reactions, as these have no radiological hazard and La(III) is diamagnetic, providing NMR spectra that are often more easily interpreted than 5f^3 U(III) [3–7]. Additionally, La(III) is a reasonable surrogate for U(III) due to their comparable ionic radii [6-coordinate, La(III) = 1.032 Å, U(III) = 1.025 Å] [24]. It is noteworthy that on one occasion during the synthesis of **3-U,** we observed several crystals of the U(IV) complex [U{tacn(SiMe$_2$NC$_6$H$_4$Me-4)$_3$}(I)] (**5**), which we attribute to the presence of traces of UI$_4$, but the low yield precluded solution phase characterization (see below). Instead of optimizing conditions for the synthesis of **5**, we decided to target analogous U(IV) chloride complexes, as straightforward salt metathesis routes to [U{tacn(SiMe$_2$NPh)$_3$}(Cl)] have been reported previously [10]. By adapting these procedures, the separate reactions of UCl$_4$ [25,26] with **1-K$_3$** and **2-K$_3$** gave the U(IV) complexes [U{tacn(SiMe$_2$NC$_6$H$_4$Me-4)$_3$}(Cl)] (**6**) and [U{tacn(SiMe$_2$NC$_6$H$_3$Me$_2$-3,5)$_3$}(Cl)] (**7**) in poor yields, following work-up and recrystallization from THF or DME, respectively (Scheme 2). We found that **6** and **7** could also be synthesized by the respective oxidation of **3-U** or **4-U** with excess ^{t}BuCl. This oxidative route gave improved yields of **6** and **7** over salt metathesis from UCl$_4$. We anticipate that the U(III) complexes **3-U** and **4-U** could give rich reactivity with small molecules and unsaturated organic compounds, as previously seen for similar tripodal U(III) complexes [3–7]; however, we were unable to isolate any uranium-containing products from the separate 1:1 reactions of **4-U** with either benzophenone or 4,4′-bipyridine in toluene. Since [U{tacn(SiMe$_2$NPh)$_3$}] has been shown to react with elemental sulfur [17], and the 2e$^-$ oxidation reactions of other tripodal U(III) complexes have been shown to give U(V) products [3–7], we attempted the synthesis of terminal U(V) oxo complexes by the separate reactions of **3-U** with pyridine *N*-oxide in toluene and **4-U** with 4-methyl morpholine *N*-oxide in THF; no products could be identified from either of these reaction mixtures.

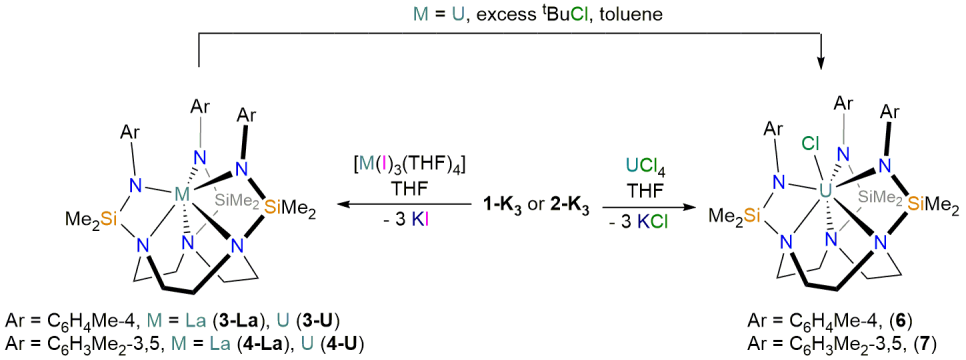

Scheme 2. Synthesis of complexes **3-M**, **4-M**, **6** and **7** (M = La, U).

2.2. NMR and IR Spectroscopy

NMR spectra are presented in the ESI Figures S13–S42. The ^{1}H and ^{13}C{^{1}H} NMR spectra of **1-H$_3$** in C_6D_6 indicate that approximate C_3 symmetry was present on the NMR timescale at 298 K. One signal was observed for each proton environment in the ^{1}H NMR spectrum apart from the *para*-Me resonances, where two signals were observed in a 3:6 ratio (δ_H: 2.11 and 2.20 ppm). The three NH protons were obscured by the broad multiplets of the tacn protons (δ_H: 2.98–3.19 ppm). Similar features were observed for **2-H$_3$**, though with the *meta*-Me resonances in a 12:6 ratio (δ_H: 2.23 and 2.24 ppm) in the ^{1}H NMR spectrum. In both **1-H$_3$** and **2-H$_3$** there are also more Ar-*H* resonances than would be expected from ideal C_3 symmetry, and this deviation is tentatively attributed to conformational rigidity of the tacn ring in solution rendering the CH_2 protons diastereotopic. The low solubility of **1-K$_3$** and **2-K$_3$** in benzene and toluene necessitated the employment of deuterated THF for NMR spectroscopy, precluding accurate integration of the proton THF resonances to validate elemental analysis data. The addition of more polar solvents to **1-K$_3$** and **2-K$_3$,** such as pyridine, lead to decomposition. The doubling of the number of resonances in the ^{13}C and ^{29}Si NMR spectra of **1-K$_3$** (δ_{Si}: −18.48 and −15.33 ppm) and **2-K$_3$** (δ_{Si}: −17.88 and −14.74 ppm) compared to the parent anilines **1-H$_3$** (δ_{Si}: −8.02 ppm) and **2-H$_3$** (δ_{Si}: −7.97 ppm) indicates that either coordinated THF reduced these systems to approximate C_s symmetry or that two different approximately C_3 symmetric complexes formed in solution. The former interpretation is the most plausible, as coordinating solvents should disfavor oligomerization.

The most noteworthy difference between the ^{1}H NMR spectra of **3-M** and **4-M** and their parent proligands is that the tacn methylene group signals split into two multiplets with AA′BB′ patterns and a relative intensity of 1:1 upon complexation. This pattern of signals is due to a significant deviation from ideal C_3 symmetry and fluxional behavior, and was previously seen for [M{tacn(SiMe$_2$NPh)$_3$}] (M = Y, Eu, Yb, U) and [La{tacn(SiMe$_2$NPh)$_3$}(THF)] by Marques and co-workers [16]. Following variable temperature ^{1}H NMR spectroscopy experiments on those literature complexes, the authors postulated that the two N_3 vertices of an approximate trigonal prism twist with respect to each other with a concomitant inversion of the tacn chelate rings; thus, we infer that similar processes are in operation for **3-M** and **4-M**. As expected, the ^{1}H NMR spectra of **3-U** and **4-U** are paramagnetically shifted, with signals from −30 to +10 ppm that show significant line broadening [27]. The ^{1}H NMR spectra of **6** and **7** displayed similar features to those of **3-U** and **4-U,** but the signals were broadened to a greater extent, with some FWHM values being as high as 1200 Hz for **6**, and the aromatic ring protons of **7** were not observed. The bulk features of these spectra are similar to those previously seen for [U{tacn(SiMe$_2$NPh)$_3$}(Cl)] [16]. Only one resonance was seen for the methylene groups in the ^{13}C{^{1}H} NMR spectra of **3-La** and **4-La**, but no signals could be observed in the ^{13}C{^{1}H} NMR spectra of **3-U**, **4-U**, **6** and **7** due to paramagnetism. The ^{29}Si{^{1}H} NMR spectra of **3-La** (δ_{Si}: −5.10 ppm) and **4-La** (δ_{Si}: −5.18 ppm) are deshielded compared to **1-H$_3$** and **2-H$_3$**; whilst no signals were seen for the U(IV) complexes **6** and **7**, the U(III) complexes exhibited remarkably shielded resonances (δ_{Si}: −263.80 ppm, **3-U**; −270.90 ppm, **4-U**) that to the best of our knowledge are the most negative values reported for any U(III) complex to date [28].

The FTIR spectra of all complexes containing {tacn(SiMe$_2$NAr)$_3$} scaffolds exhibit strong absorptions at $\tilde{\nu}$ ~ 1600 cm^{-1} due to the substituted anilide groups, as has been seen by other authors for f-block complexes containing {tacn(SiMe$_2$Nar)$_3$} [16–20]. In addition, **1-H$_3$** ($\tilde{\nu}$ = 3406 cm^{-1}) and **2-H$_3$** ($\tilde{\nu}$ = 3404 and 3377 cm^{-1}) exhibit N–H stretching absorptions, as does {tacn(SiMe$_2$HNHPh)$_3$} ($\tilde{\nu}$ = 3381 cm^{-1}) [16].

2.3. NIR/Vis/UV Spectroscopy

The electronic absorption spectra of **3-U**, **4-U**, **6** and **7** were recorded as 0.5 mM toluene solutions (Figure 1). The similar spectra of the pale green U(IV) complexes **6** and **7** are dominated by intense charge transfer bands in the UV region that tail into the visible region, and

are otherwise essentially featureless. The charge transfer bands are less prominent at higher energy for red **3-U** and **4-U** solutions, as they both exhibit a series of strong absorptions with shoulders in the visible region ($\widetilde{\nu}_{max}$, cm^{-1} (ε, M^{-1} cm^{-1}): ~17,000 (~628, **3-U**; ~692, **4-U**); ~20,000 (~1,444, **3-U**; ~1,758, **4-U**); ~23,000 (~1,308, **3-U**; ~1,612, **4-U**)) that are mainly assigned as $5f^26d^1 \leftarrow 5f^3$ transitions, consistent with U(III) centers [6]. In the NIR region, **3-U** and **4-U** exhibit nearly identical series of weak absorptions ($\varepsilon < 250$ M^{-1} cm^{-1}) that are assigned as 5f ← 5f transitions with intensities that are typical of U(III) complexes [29].

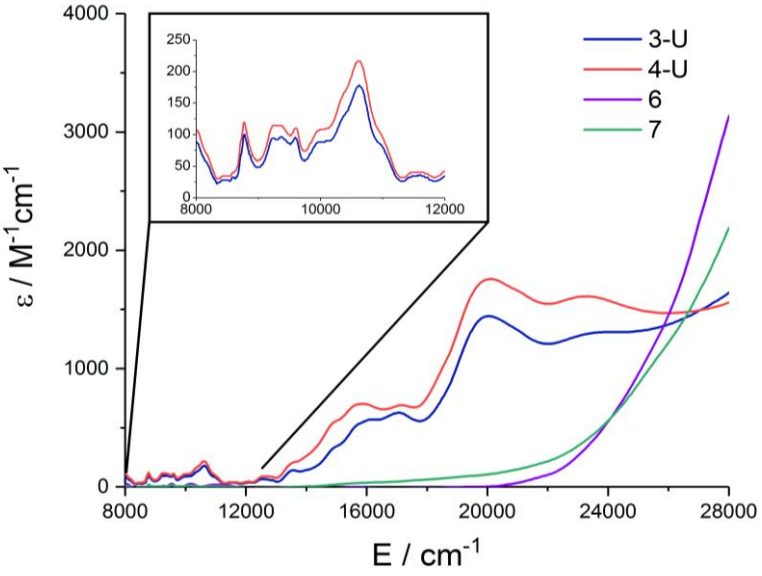

Figure 1. Electronic spectra of **3-U**, **4-U**, **6** and **7** in toluene (0.5 mM) at 8000–28,000 cm^{-1}.

2.4. Structural Characterization

The molecular structures of **3-M·0.5C$_7$H$_8$**, **4-M**, **5**, **6·THF** and **7** were determined by single-crystal X-ray diffraction (selected bond lengths and angles are listed in Table 1, and supporting crystallographic information is compiled in the ESI Tables S1 and S2). The structures of **3-U·0.5C$_7$H$_8$**, **4-U**, **6·THF** and **7** are shown in Figures 2 and 3. As **3-La·0.5C$_7$H$_8$** and **4-La** are structurally analogous with **3-U·0.5C$_7$H$_8$** and **4-U**, respectively, these are discussed together with U(III) congeners for brevity; and their structures are depicted in the ESI together with **5**, which shows similar features to **6·THF** (Figures S1–S3).

There are two independent complex molecules in the unit cells of **3-M·0.5C$_7$H$_8$**. This was seen previously for [U{tacn(SiMe$_2$NPh)$_3$}]·0.5C$_7$H$_8$ and was attributed to the presence of two isomers [16]. As the metrical parameters of the isomers are similar, we describe one of the molecules of **3-M** here. In each case, the metal centers exhibit approximate trigonal prismatic geometries defined by approximately parallel and near-eclipsed amine (N_1-N_3) and anilide (N_4-N_6) planes, and lie much closer to the anilide [M···N_4-N_6 (Å): 0.468(2) (**3-La**); 0.513(4) (**3-U**)] than the amine [M···N_1-N_3 (Å): 2.064(2) (**3-La**); 2.030(4) (**3-U**)] planes. Despite differences in 6-coordinate ionic radii (La(III) = 1.032 Å, U(III) = 1.025 Å) [18], significant disorder in the dataset for **3-U** led to poor resolution of M–N distances, to the extent that these were within statistical error of the corresponding distances in **3-La**. The bulk features of **4-M** are similar to those of their **3-M** analogs; for example, in **4-U** the position of the uranium center within the N_6 prism [U···N_4-N_6: 0.509(8) Å; U···N_1-N_3: 2.002(8) Å; mean U–N_{amine}: 2.63(2) Å; U–$N_{anilide}$: 2.36(2) Å] is almost identical to those seen for [U{tacn(SiMe$_2$NPh)$_3$}] [16] and **3-U** (see Figure S4 for space-filling representations of [U{tacn(SiMe$_2$NPh)$_3$}], **3-U** and **4-U** viewed along the approximate C_3 axes above the *N*-aryl rings).

Table 1. Selected bond lengths (Å) and angles (°) for **3-M·0.5C$_7$H$_8$**, **4-M, 5**, **6·THF** and **7** (M = La, U; X = Cl, I). Symmetry operations to generate equivalent atoms: i 1–*x*, +*y*, +*z*; ii = +*x*, $\frac{1}{2}$–*y*, +*z*.

Complex	M–N$_{amine}$	M–N$_{anilide}$	N–M–N$_{amine}$	N–M–N$_{anilide}$	M–X
3-La·0.5C$_7$H$_8$	2.705(3) 2.705(3) 2.654(3)	2.395(3) 2.414(3) 2.436(3)	66.21(8) 68.00(9) 67.54(7)	120.06(9) 113.46(8) 115.46(10)	-
3-U·0.5C$_7$H$_8$	2.637(9) 2.659(8) 2.658(6)	2.381(8) 2.364(7) 2.396(10)	68.2(2) 67.4(3) 67.5(3)	119.0(3) 116.6(3) 110.8(3)	-
4-La	2.674(2) 2.676(3) 2.707(3)	2.421(3) 2.426(2) 2.400(3)	67.80(7) 67.09(8) 68.02(8)	115.74(9) 116.64(9) 115.99(8)	-
4-U	2.616(12) 2.646(10) 2.63(2)	2.348(10) 2.31(2) 2.418(14)	68.2(4) 68.3(4) 68.6(5)	117.9(6) 115.6(4) 112.9(5)	-
5	2.74(4) 2.67(2) 2.59(4)	2.36(2) 2.32(2) 2.32(2) [i]	66.0(1) 64.8.(8) 67.7(9)	96.6(4) 154.5(7) 96.6(4) [i]	3.143(2)
6·THF	2.659(8) 2.683(7) 2.635(7)	2.285(7) 2.295(8) 2.327(8)	66.6(3) 67.1(2) 66.0(2)	95.4(3) 160.3(3) 94.1(3)	2.706(3)
7	2.69(2) 2.667(7) 2.62(2)	2.305(5) 2.286(5) 2.305(5) [ii]	66.8(5) 67.8(5) 65.4(6)	95.77(10) 158.2(3)(10) 95.77(10) [ii]	2.687(2)

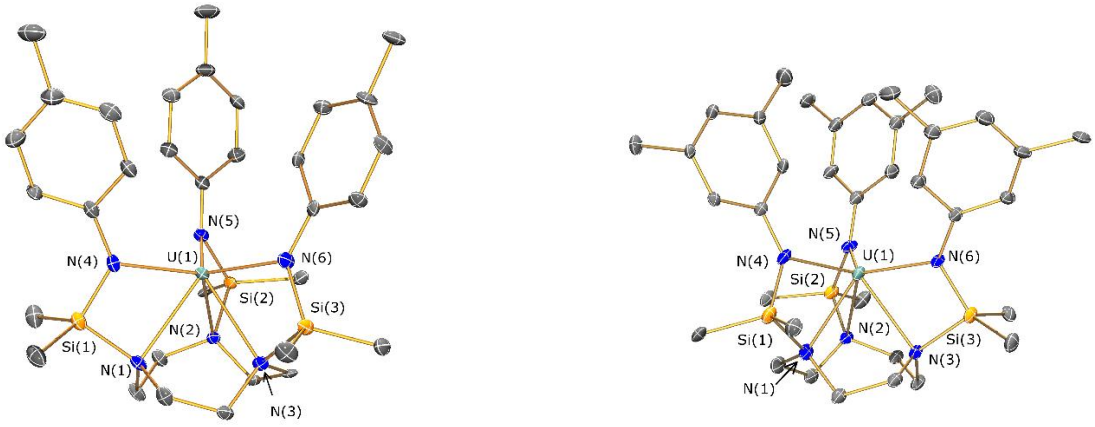

(**a**) (**b**)

Figure 2. Molecular structures of (**a**) [U{tacn(SiMe$_2$NC$_6$H$_4$Me-4)$_3$}] (**3-U·0.5C$_7$H$_8$**) and (**b**) [U{tacn(SiMe$_2$NC$_6$H$_3$Me$_2$-3,5)$_3$}] (**4-U**) with selective atom labelling. Displacement ellipsoids set at 30% probability level; hydrogen atoms and lattice toluene were omitted for clarity.

Although **5–7** all crystallize in different space groups and **6·THF** additionally incorporates a molecule of THF in the unit cell, the metrical parameters of **5–7** are similar to those of [U{tacn(SiMe$_2$NPh)$_3$}(Cl)]. Whilst [U{tacn(SiMe$_2$NPh)$_3$}(I)] was also synthesized previously by oxidation of [U{tacn(SiMe$_2$NPh)$_3$}] with iodine, its solid state structure was not reported [16]. As with [U{tacn(SiMe$_2$NPh)$_3$}(Cl)] [16], the positions of the donor atoms in **5–7** can be described as bicapped trigonal bipyramids with one anilide and two amine donors forming the equatorial plane; the halide and remaining amine at the axial positions [N(1)–U(1)–X(1): 169.7(5)° (**5**); 171.7(2)° (**6**); 171.7(2)° (7)]; and the other two anilides capping two faces near the halide apex. The uranium centers are situated above the N$_3$-tacn plane [U···N$_1$-N$_3$ (Å): 1.04(2) (**5**); 1.021(5) (**6**); 1.011(6) (**7**)] such that for **6** and **7** the apical U–N distances [2.683(7) Å (**6**); 2.667(9) Å (**7**)] are similar to the U–Cl distances [2.706(3) Å (**6**); 2.687(2) Å (**7**)].

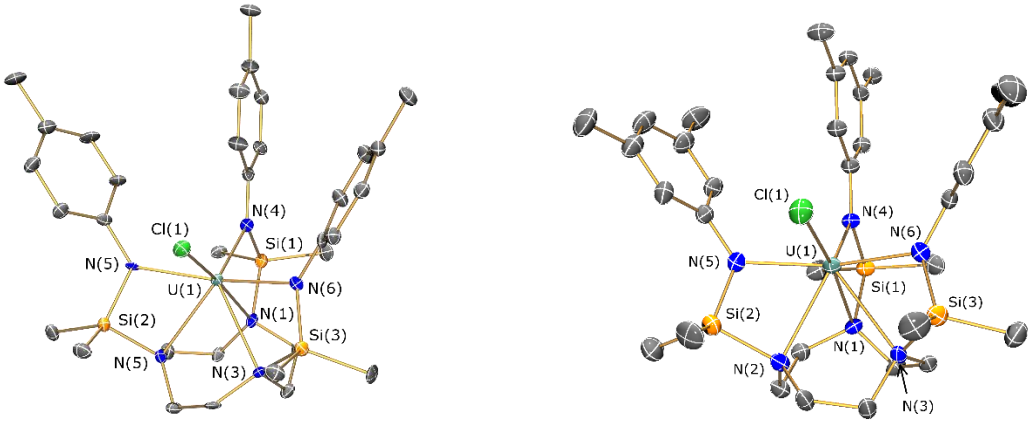

(**a**) (**b**)

Figure 3. Molecular structures of (**a**) [U{tacn(SiMe$_2$NC$_6$H$_4$Me-4)$_3$}(Cl)] (**6**·**THF**) and (**b**) [U{tacn(SiMe$_2$NC$_6$H$_3$Me$_2$-3,5)$_3$}(Cl)] (**7**) with selective atom labelling. Displacement ellipsoids set at 30% probability level; hydrogen atoms omitted for clarity.

2.5. Magnetism and EPR Spectroscopy

Solution magnetic susceptibility measurements of U(III) and U(IV) complexes, measured in C_6D_6 at 298 K using the Evans method [30], gave similar χT values: **3-U** (1.05 cm^3 K mol^{-1}), **4-U** (0.95 cm^3 K mol^{-1}), **6** (0.98 cm^3 K mol^{-1}) and **7** (1.13 cm^3 K mol^{-1}). Whilst these molar susceptibilities are all lower than the free ion values [U(III) 5f^3 ^{4}I$_{9/2}$ = 1.70 cm^3 K mol^{-1}; U(IV) 5f^2 ^{3}H$_4$ = 1.60 cm^3 K mol^{-1}], this was expected, as not all crystal field levels are thermally occupied at this temperature [31]. Indeed, the values obtained are around the middle of the previously reported ranges for monometallic U(III) (0.38–1.81 cm^3 K mol^{-1}) and U(IV) (0.48–1.34 cm^3 K mol^{-1}) complexes [32]. Variable temperature solid state magnetic susceptibility measurements for powdered samples of **3-U**, **4-U**, **6** and **7** suspended in eicosane were recorded using a SQUID from 300–2 K (ESI Figures S5–S9). At 300 K, the magnetic susceptibility temperature products [χT (cm^3 K mol^{-1}): 0.84 (**3-U**); 0.70 (**4-U**); 0.60 (**6**); 0.80 (**7**)] were consistently lower than solution values by 0.2–0.4 cm^3 K mol^{-1}, but such discrepancies should be expected from changes in phase, together with variable errors associated with sample masses and diamagnetic corrections. At 298 K, the solid state χT value for **3-U** is similar to that previously reported for [U{tacn(SiMe$_2$NPh)$_3$}] (0.94 cm^3 K mol^{-1}) [19]. U(IV) complexes **6** and **7** showed χT temperature dependence that correlates with metal oxidation state, tending towards zero at low temperatures due to a non-magnetic singlet ground state [χT (cm^3 K mol^{-1}) at 2 K: 0.07 (**6**); 0.10 (**7**)]. The U(III) complexes, **3-U** and **4-U**, reached values that are higher than those of **6** and **7** [χT (cm^3 K mol^{-1}) at 2 K: 0.20 (**3-U**); 0.15 (**4-U**)], but did not reach their low temperature limit, which suggests occupation of low lying excited states [33–35]. This is consistent with the magnetization data (see below).

The U(III) formulations of **3-U** and **4-U** were confirmed by X- and Q-band EPR spectroscopy on powdered samples at 5 K (X-band spectrum of **4-U** shown in Figure 4a; see ESI Figures S10–S12 for other spectra). The spectra of **4-U** are characteristic of an effective spin $\frac{1}{2}$, consistent with a Kramers doublet, with g_{eff} = 2.80, 2.37 and 1.17. Complex **3-U** shows greater rhombicity in the g_{eff} values, but they are complicated by what appears to be an impurity, and we were unable to model these spectra. As U(III) complexes can exhibit single-molecule magnet (SMM) behavior in small applied magnetic fields [33–35], we investigated the dynamic magnetic properties of **3-U** and **4-U**. Both complexes exhibited hysteresis at 1.8 K, but this was more pronounced for **3-U** (Figure 4b) than for **4-U** (see ESI Figure S6d); in both cases, magnetic saturation was not achieved at 7 T, the physical limit of the magnetometer. Ac susceptibility measurements were performed on **3-U** and **4-U** under an applied dc field of 600 G at 1.8 K. Whilst **3-U** did not exhibit in-phase or out-of-phase components, **4-U** displayed clear frequency dependent behavior (Figure 4c,d).

An Arrhenius plot of the data gave an effective energy barrier to magnetic reversal, U_{eff}, of 16.2 (±0.8) K (see ESI Figure S9).

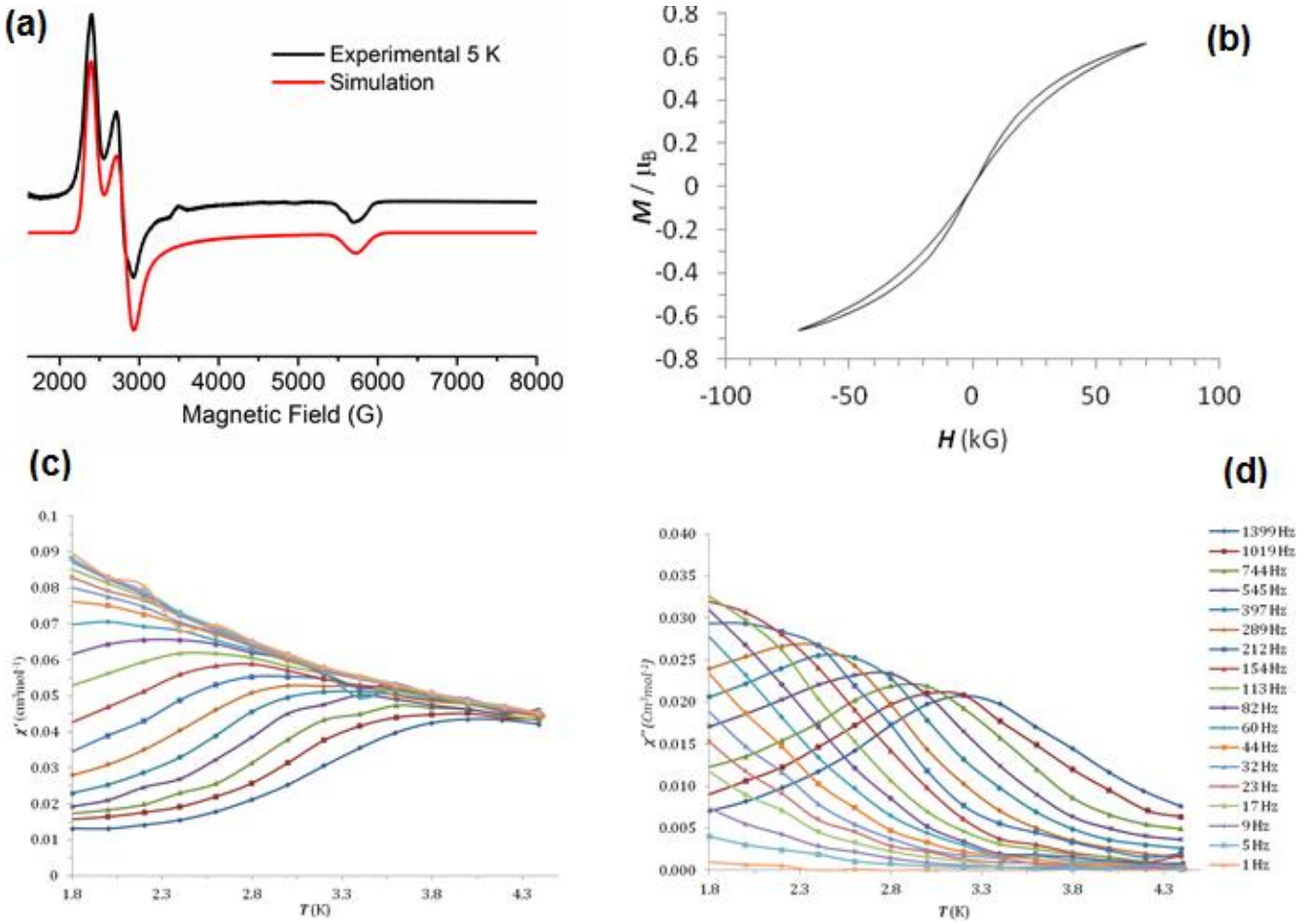

Figure 4. (**a**) (black) Powder X-band EPR spectrum of **4-U** at 5 K, and (red) its simulation with g_{eff} = 2.80, 2.27 and 1.17. (**b**) Magnetization (M) hysteresis of **3-U** at 1.8 K, sweep rate 13 G s^{-1}. (**c**) In phase (χ′) and (**d**) out of phase (χ″) components of the ac susceptibility of **4-U** in an applied field of 600 G and an oscillating field of 1.55 G at 1.8 K.

3. Discussion

Comparisons of the multinuclear NMR spectra of **3-M** and **4-M** with each other and analogous M(III) {tacn($SiMe_2NPh)_3$} complexes [16] indicate that minor variations in anilide substitution patterns do not considerably affect dynamic solution behavior. The solubility and solution stability of complexes also did not appear to vary significantly upon ligand substitution. In the solid state, the single-crystal XRD data show that most of the metrical parameters of **3-U** (e.g., mean U–N_{amine}: 2.651(13) Å; U–$N_{anilide}$: 2.38(2) Å) are nearly identical to those reported previously for [U{tacn($SiMe_2NPh)_3$}] [U···N_1–N_3: 0.52 Å; U···N_4–N_6: 2.02 Å; mean U–N_{amine}: 2.66(3) Å; U–$N_{anilide}$: 2.35(3) Å] [10]. However, the ranges of $N_{anilide}$–U–$N_{anilide}$ [**3-U**: 110.8(3)–119.0(3)°; **4-U**: 112.9(5)–117.9(6)°] and U–$N_{anilide}$–C_{ipso} [**3-U**: 115.8(6)–127.0(7)°; **4-U**: 117.7(10)–125.9(9)°] angles are greater for **3-U** than for **4-U**, consistent with nearer-axial EPR spectra of **4-U,** and showing that substitution of the *N*-aryl groups can influence both the shape and size of the apical channel in the solid state. Structural differences are even more pronounced for the La(III) homologs **3-La** and **4-La**, which do not contain bound THF molecules, in contrast with the 7-coordinate La(III) unsubstituted analog [La{tacn($SiMe_2NPh)_3$}(THF)] [16]. This change in coordination number leads to more significant changes in metrical parameters; for example, the mean La–N_{amine} [2.685(5) Å] and La–$N_{anilide}$ [2.415(5) Å] distances for **3-La** differ markedly from [La{tacn($SiMe_2NPh)_3$}(THF)] [mean La–N_{amine}: 2.751(8) Å; La–$N_{anilide}$: 2.453(8) Å] [16].

The main differences between the solid state structures of the U(IV) and U(III) complexes reported herein are that the approximate C_3 symmetry is broken upon oxidation of the metal center, with the seventh coordination site being occupied by a halide ion. Despite the increase in metal oxidation state, the respective mean $U–N_{anilide}$ and $U–N_{amine}$ distances of **5–7** were similar to those seen for **3-U** and **4-U**, which we attribute to the considerable rearrangement of metal coordination spheres. This facile reorganization is a distinguishing feature of the flexible $SiMe_2$ linkers in {tacn($SiMe_2NAr)_3$} frameworks [16–20] compared to the more rigid tethered aryloxides in {tacn($CH_2ArO)_3$)}, where oxidation of U(III) starting materials to U(IV/V/VI) products has been shown to proceed with retention of approximate C_3 symmetry [3–7]. As {tacn($SiMe_2NAr)_3$} scaffolds readily reorganize to accommodate an additional donor atom, we posit that THF may bind to **3-M** and **4-M** in solution, but that this molecule is readily displaced upon exposure to vacuum during work-up and recrystallization. A detailed reactivity study would be required to determine if the fluxionality of {tacn($SiMe_2NAr)_3$} frameworks in solution reduces the steric effect of anilide substituents compared to analogous R-group variation in more rigid tripodal ligands.

A comparison of the characterization data for the U(III) complexes **3-U**, **4-U** and [U{tacn($SiMe_2NPh)_3$}] [16,19] indicates that minor changes in the anilide substituents can lead to subtle changes in the physicochemical properties of complexes. The UV/Vis/NIR electronic absorption spectrum of **4-U** shows more intense absorption intensities than that of **3-U**. To the best of our knowledge, the corresponding data for [U{tacn($SiMe_2NPh)_3$}] have not been published. Similarly, as we were only able to model the EPR spectra of **4-U** (g_{eff} = 2.80, 2.37 and 1.17) and we could not find literature EPR data for [U{tacn($SiMe_2NPh)_3$}], we cannot make a detailed comparison of structurally similar complexes, though we note that g_{eff} =3.54(5), 2.042(4) and 1.66(5) were determined for [U{tacn($SiMe_2NPh)_3$}($OPPh_3$)], where the phosphine oxide occupies the apical position [20]. We previously reported the EPR spectra of the planar U(III) tris-amide [U{$N(SiBuMe_2)_2\}_3$] [36]. They gave g_{eff} (=3.55, 2.97, 0.55) that approach those expected for the $|m_J| = 1/2$ doublet of a $^4I_{9/2}$ term (3.65, 3.65, 0.73), which is stabilized by the in-plane crystal field. For **4-U**, the uranium center is close to the anilide N_3 plane, which likewise would stabilize the $|m_J| = 1/2$ state, but the out-of-plane crystal field arising from the three amine donors leads to significant mixing. Assuming three-fold symmetry, the $m_J = \pm 1/2$ state can mix with both the $\pm 5/2$ and $\pm 7/2$ states (assuming a $^4I_{9/2}$ term) leading to very different g-values. A similar result was concluded for the parent [U{tacn($SiMe_2NPh)_3$}], where crystal field calculations gave a very mixed ground state comprising almost equal fractions of $|m_J| = 5/2$ and $1/2$ (EPR spectra were not reported) [19]. Finally, we note that the SMM behavior of U(III) {tacn($SiMe_2NAr)_3$} complexes appears to be quite sensitive to anilide substituent variation. No effective barrier to magnetic reversal was seen for [U{tacn($SiMe_2NPh)_3$}] [19] and **3-U,** whereas U_{eff} = 16.2 ($\pm$0.8) K for 4-**U** is similar to values reported previously for U(III) complexes [33–35]; e.g., [U{tacn($SiMe_2NPh)_3$}($OPPh_3$)], U_{eff} = 21.9(7) K [20].

4. Materials and Methods

General Information

Caution—uranium-238 ($t_{1/2}$ = 4.47 × 10^9 years) is a weak α-emitter; therefore, all manipulations should be performed in suitable laboratories that have been designated for radiochemical use, and α-counting equipment should be available. All manipulations were carried out using standard Schlenk and glove box techniques under an atmosphere of dry argon. THF, toluene, *n*-hexane and DME were dried by refluxing over potassium. All solvents were stored over K mirrors (with the exception of THF and DME, which were stored over activated 4 Å molecular sieves), and were degassed prior to use. Deuterated solvents were dried over K, degassed by three freeze-pump-thaw cycles and stored under Ar. tacn($SiMe_2Cl)_3$ [21], [$La(I)_3(THF)_4$] [22], [$U(I)_3(THF)_4$] [23] and UCl_4 [25,26] were prepared according to literature procedures, and all other reagents were purchased. *p*-Toluidine was dried for 4 h under vacuum before use, whilst 3,5-dimethylaniline was refluxed over CaH_2 and distilled.

KH and NaH were obtained as suspensions in mineral oil and were washed three times with *n*-hexane before use.

^{1}H, ^{13}C{^{1}H} and ^{29}Si{^{1}H} NMR spectra were recorded on a Bruker Avance III 400 MHz spectrometer operating at 400.1, 100.6 and 79.5 MHz, respectively; chemical shifts are quoted in ppm and are relative to TMS. FTIR spectra were recorded as Nujol mulls in KBr discs on a Perkin Elmer Spectrum RX1 spectrometer (Perkin Elmer, Waltham, MA, USA). Elemental microanalyses were carried out by Stephen Boyer at the Microanalysis Service, London Metropolitan University, or by Martin Jennings and Anne Davies at The University of Manchester. Low carbon values were consistently obtained in elemental analyses of **2-K$_3$**, **3-La** and **4-La**. We attribute this observation to silicon carbide formation, as <5% protic impurities were observed by ^{1}H NMR spectroscopy, and we note that low C values were intermittently obtained in microanalysis experiments for f-element complexes of the related ligand {tacn(SiMe$_2$NPh)$_3$} [16]. UV-Vis-NIR spectroscopy was performed on samples in Youngs tap appended 10 mm pathlength quartz cuvettes on an Agilent Technologies Cary Series UV-Vis-NIR Spectrophotometer (Agilent Technologies, Santa Clara, CA, USA) from 175–3300 nm. X- and Q-band EPR spectroscopy was performed on powdered samples in quartz tubes at 5 K sealed under vacuum. Magnetic measurements were made using a Quantum Design MPMS-XL7 SQUID magnetometer on ground crystalline samples suspended in eicosane in borosilicate tubes sealed under vacuum.

Crystals of **3-M·0.5C$_7$H$_8$**, **4-M** (M = La, U) and **5–8** were examined on a Rigaku Oxford Diffraction SuperNova CCD area detector diffractometer (Rigaku, Tokyo, Japan) using mirror-monochromated Mo Kα radiation (λ = 0.71073 Å). Intensities were integrated from data recorded on 1° frames by ω rotation. Cell parameters were refined from the observed positions of all strong reflections in each data set. A Gaussian grid face-indexed absorption correction with a beam profile correction was applied [37]. The structures were solved variously by direct and heavy atom methods using *SHELXS* [38] or *SHELXT* [39] and were refined by full-matrix least-squares on all unique F^2 values [38], with anisotropic displacement parameters for all non-hydrogen atoms, and with constrained riding hydrogen geometries; U_{iso}(H) was set at 1.2 (1.5 for methyl groups) times U_{eq} of the parent atom. The largest features in final difference syntheses were close to those of heavy atoms and were of no chemical significance. *CrysAlisPRO* [37] was used for control and integration, *SHELX* [38] and was employed through *OLEX2* [40] for structure solution and refinement and *ORTEP-3* [41] and *POVRAY* [42] were used for molecular graphics.

Synthesis of {tacn(SiMe$_2$NHC$_6$H$_4$Me-4)$_3$} (**1-H$_3$**): *p*-toluidine (5.36 g, 50.0 mmol) was added to a slurry of NaH (2.16 g, 90.0 mmol) in THF (30 mL) and was heated to 50 °C for 18 h. The resultant brown suspension was allowed to cool to room temperature and filtered. The dark brown supernatant was added dropwise to a solution of tacn(SiMe$_2$Cl)$_3$ (6.30 g, 15.5 mmol) in toluene (50 mL) at −78 °C, allowed to slowly warm to room temperature and stirred for 18 h. Volatiles were removed under reduced pressure and the resultant yellow oil was extracted with hexane (3 × 50 mL). The solvent was removed under reduced pressure to give crude **1-H$_3$** as a viscous yellow oil (7.56 g, 79%), which was used without further purification. Anal. Calcd. for C$_{33}$H$_{54}$N$_6$Si$_3$: C, 64.02; H, 8.79; N, 13.58. Found: C, 64.22; H, 8.94; N, 13.44. ^{1}H NMR (C$_6$D$_6$, 298 K): δ = 0.21 (18H, s, Si(C*H*$_3$)$_2$), 2.11 (3H, s, Ar-C*H*$_3$), 2.20 (6H, s, Ar-C*H*$_3$), 2.98–3.19 (15H, br m, NC*H*$_2$ and N*H*), 6.61 (d, 4H, J_{HH} = 8.0 Hz, Ar-*H*), 7.01 (m, 6H, J_{HH} = 8.0 Hz, Ar-*H*), 7.13 (2H, br m, J_{HH} = 8.0 Hz, Ar-*H*). ^{13}C{^{1}H} NMR (C$_6$D$_6$, 298 K): δ = –0.69 (Si(*C*H$_3$)$_2$), 20.99 (Ar-*C*H$_3$), 50.96 (N*C*H$_2$), 117.25 (*p*-Ar-*C*H), 127.25 (Ar-*C*H), 130.45 (Ar-*C*H), 145.33 (*ipso*-Ar-*C*). ^{29}Si{^{1}H} NMR (C$_6$D$_6$, 298 K): δ = –8.02 (*Si*Me$_2$). FTIR (Nujol, $\tilde{\nu}$/cm^{-1}): 3406 (m), 1614 (s), 1512 (w), 1285 (s), 1167 (m), 1148 (m), 1109 (m), 995 (s), 968 (s), 895 (s), 692 (m), 638 (m).

Synthesis of {tacn(SiMe$_2$NKC$_6$H$_4$Me-4)$_3$}·2THF (**1-K$_3$**): **1-H$_3$** (7.56 g, 12.2 mmol) was dissolved in THF (20 mL) and added dropwise to a suspension of KH (2.79 g, 70 mmol) in THF (10 mL) at −78 °C. The reaction mixture was allowed to warm to room temperature, heated to 50 °C overnight, allowed to cool and filtered. Volatiles were removed under reduced pressure and the resultant solid was washed with hexane (20 mL) and dried in vacuo

to yield **1-K$_3$** as an off-white powder (6.10 g, 62%). Anal. Calcd. for $C_{41}H_{67}K_3N_6O_2Si_3$: C, 56.11; H, 7.70; N, 9.52. Found: C, 55.95; H, 7.80; N, 9.47. ^{1}H NMR (C_4D_8O, 298 K): δ = 0.01 (s, 12H, Si(CH_3)$_2$), 0.11 (s, 6H, Si(CH_3)$_2$), 1.78 (m, 4H, OCH$_2$CH_2), 2.05 (s, 9H, Ar-CH_3), 2.72–2.91 (m, 12H, NCH_2), 3.62 (m, 4H, OCH_2CH$_2$), 6.23 (d, 4H, J_{HH} = 8.0 Hz, Ar-*H*), 6.56 (d, 6H, J_{HH} = 8.0 Hz, Ar-*H*), 6.63 (d, 2H, J_{HH} = 8.0 Hz, Ar-*H*). ^{13}C{^{1}H} NMR (C_4D_8O, 298 K): δ = 0.22 (Si(CH$_3$)$_2$), 0.39 (Si(CH_3)$_2$), 20.74 (Ar-CH$_3$), 20.83 (Ar-CH$_3$), 26.55 (OCH$_2$CH$_2$), 49.19 (NCH$_2$), 49.32 (NCH$_2$), 68.39 (OCH$_2$CH$_2$), 117.46 (*p*-Ar-*C*), 118.82 (*p*-Ar-*C*), 122.23 (Ar-CH), 122.82 (Ar-CH), 130.66 (Ar-CH), 130.90 (Ar-CH), 160.09 (*ipso*-Ar-*C*), 160.94 (*ipso*-Ar-*C*). ^{29}Si DEPT NMR (C_4D_8O, 298 K): δ = –18.48, –15.33 (*Si*Me$_2$). FTIR (Nujol, $\tilde{\nu}$/cm^{-1}): 1595 (s), 1172 (m), 1057 (m), 995 (s), 955 (m), 893 (m), 870 (m), 756 (m), 683 (w), 635 (w).

Synthesis of {tacn(SiMe$_2$NC$_6$H$_3$Me-3,5)$_3$} (**2-H$_3$**): 3,5-dimethylaniline (7.23 g, 59.7 mmol) was added to a slurry of NaH (3.46 g, 144.0 mmol) in THF (30 mL) and heated to 50 °C for 18 h. The resultant brown suspension was allowed to cool to room temperature and filtered. The dark brown supernatant was added dropwise to a solution of tacn(SiMe$_2$Cl)$_3$ (7.51 g, 18.5 mmol) in toluene (50 mL) at –78 °C, allowed to slowly warm to room temperature and stirred for 18 h. Volatiles were removed under reduced pressure and the resultant yellow oil was extracted with hexane (3 × 50 mL). The solvent was removed under reduced pressure to give crude **2-H$_3$** as a viscous yellow oil, which was used without further purification (10.40 g, 85%). Anal. Calcd. for $C_{36}H_{60}N_6Si_3$: C, 65.40; H, 9.15; N, 12.71. Found: C, 64.94; H, 9.14; N, 12.38. ^{1}H NMR (C_6D_6, 298 K): δ = 0.23 (s, 12H, s, Si(CH_3)$_2$), 0.27 (s, 6H, s, Si(CH_3)$_2$), 2.23 (s, 12H, Ar-CH_3), 2.24 (6H, s, Ar-CH_3), 3.02–3.25 (15H, br m, NCH_2 and N*H*), 6.32 (s, 4H, Ar-*H*), 6.35 (s, 2H, Ar-*H*), 6.45 (s, 3H, Ar-*H*). ^{13}C{^{1}H} NMR (C_6D_6, 298 K): δ = 0.68 (Si(CH$_3$)$_2$), 22.08 (Ar-CH$_3$), 51.03 (NCH$_2$), 115.35 (Ar-CH), 120.62 (Ar-CH), 138.93 (*m*-Ar-*C*), 147.70 (*ipso*-Ar-*C*). ^{29}Si{^{1}H} NMR (C_6D_6, 298 K): δ = −7.97 (*Si*Me$_2$). FTIR (Nujol, $\tilde{\nu}$/cm^{-1}): 3404 (m), 3377 (m), 1599 (s), 1406 (m), 1325 (m), 11776 (s), 1120 (s), 1109 (m), 1057 (s), 966 (m), 821 (br, s), 691 (s).

Synthesis of {tacn(SiMe$_2$NKC$_6$H$_3$Me$_2$-3,5)$_3$}·THF (**2-K$_3$**): **2-H$_3$** (10.40 g, 15.7 mmol) was dissolved in THF (20 mL) and added dropwise to a suspension of KH (2.16 g, 54.0 mmol) in THF (10 mL) at −78 °C. The reaction mixture was allowed to warm to room temperature and heated to 50 °C overnight, allowed to cool and filtered. Volatiles were removed under reduced pressure, and the resultant solid was washed with hexane (20 mL) and dried in vacuo to yield **2-K$_3$** as an off-white powder (12.50 g, 86%). Anal. Calcd. for $C_{40}H_{65}K_3N_6OSi_3$: C, 58.69; H, 7.73; N, 9.92. Found: C, 54.96; H, 7.72; N, 9.95. ^{1}H NMR (C_4D_8O, 298 K): δ = 0.04 (s, 12H, s, Si(CH_3)$_2$), 0.13 (s, 6H, s, Si(CH_3)$_2$), 1.78 (m, OCH$_2$CH_2), 2.00 (s, 12H, Ar-CH_3), 2.06 (6H, s, Ar-CH_3), 2.72-2.93 (12H, br m, NCH_2), 3.62 (m, OCH_2CH$_2$), 5.70 (s, 2H, Ar-*H*), 5.78 (s, 1H, *p*-Ar-*H*), 6.00 (s, 4H, Ar-*H*), 6.29 (s, 2H, Ar-*H*). ^{13}C{^{1}H} NMR (C_4D_8O, 298 K): δ = 0.35 (Si(CH$_3$)$_2$), 0.43 (Si(CH_3)$_2$), 22.31 (Ar-CH$_3$), 22.36 (Ar-CH$_3$), 26.55 (OCH$_2$CH$_2$), 49.16 (NCH$_2$), 49.39 (NCH$_2$), 68.39 (OCH$_2$CH$_2$), 112.52 (Ar-CH), 113.67 (Ar-CH), 120.32 (Ar-CH), 120.91 (Ar-CH), 138.34 (*m*-Ar-*C*), 138.74 (*m*-Ar-*C*), 162.82 (*ipso*-Ar-*C*), 163.25 (*ipso*-Ar-*C*). ^{29}Si DEPT NMR (C_4D_8O, 298 K): δ = –17.88, –14.74 (*Si*Me$_2$). FTIR (Nujol, $\tilde{\nu}$/cm^{-1}): 1557 (s), 1352 (m), 1240 (m), 1194 (m), 1173 (m), 1117 (m), 1057 (m), 978 (w), 916 (m), 893 (m), 843 (m), 760 (m), 654 (m).

Synthesis of [La{tacn(SiMe$_2$NC$_6$H$_4$Me-4)$_3$}] (**3-La**): THF (20 mL) was added to a pre-cooled (−78 °C) mixture of [La(I)$_3$(THF)$_4$] (0.40 g, 0.5 mmol) and **1-K$_3$** (0.44 g, 0.5 mmol). The pale yellow reaction mixture was allowed to warm to room temperature and stirred for 16 h. Volatiles were removed under reduced pressure and the residue was extracted with toluene (2 × 10 mL), reduced in volume to ca. 2 mL and stored at −30 °C overnight to give colorless crystals of **3-La·0.5C$_7$H$_8$** (0.13 g, 32%). Anal. Calcd. for $C_{33}H_{51}LaN_6Si_3 \cdot C_7H_8$: C, 56.71; H, 7.02; N, 9.92. Found: C, 51.64; H, 6.93; N, 9.54. ^{1}H NMR (C_6D_6, 298 K): δ = 0.27 (s, 18H, Si(CH_3)$_2$), 2.21 (s, 9H, Ar-CH_3), 2.23-2.34 (m, 6H, NCH_2), 2.81-2.89 (m, 6H, NCH_2), 6.64 (d, 6H, J_{HH} = 8.0 Hz, Ar-*H*), 6.98 (d, 6H, J_{HH} = 8.0 Hz, Ar-*H*). ^{13}C{^{1}H} NMR (C_6D_6, 298 K): δ = 0.80 (Si(CH$_3$)$_2$), 21.13 (Ar-CH$_3$), 48.65 (NCH$_2$), 121.04 (Ar-CH), 126.14 (*p*-Ar-*C*), 131.33 (Ar-CH), 151.10 (*ipso*-Ar-*C*). ^{29}Si{^{1}H} NMR (C_6D_6, 298 K): δ = –5.10 (s, *Si*Me$_2$). FTIR

(Nujol, $\widetilde{\nu}/cm^{-1}$): 1606 (s), 1503 (s), 1297 (m), 1178 (w), 1041 (m), 1017 (m), 958 (m), 894 (m), 816 (s), 771 (s).

Synthesis of [U{tacn(SiMe$_2$NC$_6$H$_4$Me-4)$_3$}] (**3-U**) *and [U{tacn(SiMe$_2$NC$_6$H$_4$Me-4)$_3$}(I)]* (**5**): THF (20 mL) was added to a pre-cooled (−78 °C) mixture of [U(I)$_3$(THF)$_4$] (0.45 g, 0.5 mmol) and **1-K$_3$** (0.44 g, 0.5 mmol). The dark red reaction mixture was allowed to warm to room temperature and stirred for 16 h. The volatiles were removed in vacuo and the residue was extracted with toluene (2 ×10 mL) and filtered. The solution was reduced in volume to ca. 2 mL and stored at −30 °C overnight to give dark red crystals of **3-U·0.5C$_7$H$_8$** (0.25 g, 56%). On one occasion, several crystals of **5** formed. The solid state structure of **5** was determined, but no other characterization data could be obtained due to the low yield. Data for **3-U**: Anal. Calcd. for $C_{33}H_{51}N_6Si_3U{\cdot}0.5C_7H_8$: C, 48.70; H, 6.16; N, 9.34. Found: C, 48.53; H, 6.09; N, 9.47. μ_{eff} = 2.97 μ_B (Evans method). ^{1}H NMR (C$_6$D$_6$, 298 K): δ = −30.29 (br, $\nu\frac{1}{2}$ ~ 150 Hz, 6H, NC*H*$_2$), −7.50 (br, $\nu\frac{1}{2}$ ~ 150 Hz, 6H, NC*H*$_2$), −0.65 (br, $\nu\frac{1}{2}$ ~ 20 Hz, 6H, Ar-C*H*), −0.40 (br, $\nu\frac{1}{2}$ ~ 30 Hz, 9H, Ar-C*H*$_3$), 2.67 (br, $\nu\frac{1}{2}$ ~ 30 Hz, 6H, Ar-C*H*), 7.74 (br, $\nu\frac{1}{2}$ ~ 50 Hz, 18H, Si(C*H*$_3$)$_2$). ^{13}C{^{1}H} NMR (C$_6$D$_6$, 298 K): not observed. ^{29}Si{^{1}H} NMR (C$_6$D$_6$, 298 K): δ = −263.80 (*Si*Me$_2$). FTIR (Nujol, $\widetilde{\nu}/cm^{-1}$): 1605 (s), 1506 (m), 1290 (s), 1260 (m), 1177 (m), 1034 (m), 951 (s), 912 (w), 895 (m), 862 (m), 816 (s), 770 (s).

Synthesis of [La{tacn(SiMe$_2$NC$_6$H$_3$Me$_2$-3,5)$_3$}] (**4-La**): THF (20 mL) was added to a pre-cooled (−78 °C) mixture of [La(I)$_3$(THF)$_4$] (0.40 g, 0.5 mmol) and **2-K$_3$** (0.46 g, 0.5 mmol). The pale yellow reaction mixture was allowed to warm to room temperature and stirred for 16 h. Volatiles were removed under reduced pressure and the residue was extracted with toluene (2 × 10 mL), reduced in volume to ca. 1 mL and stored at −30 °C overnight to give colorless crystals of **4-La** (0.27 g, 68%). Anal. Calcd. for $C_{36}H_{57}LaN_6Si_3$: C, 54.25; H, 7.21; N, 10.54. Found: C, 53.06; H, 7.23; N, 10.03. ^{1}H NMR (C$_6$D$_6$, 298 K): δ = 0.30 (s, 18H, s, Si(C*H*$_3$)$_2$), 2.13 (s, 18H, Ar-C*H*$_3$), 2.23-2.33 (br m, 6H, NC*H*$_2$), 2.79-2.87 (br m, 6H, NC*H*$_2$), 6.39 (s, 6H, *o*-Ar-*H*), 6.42 (s, 3H, *p*-Ar-*H*). ^{13}C{^{1}H} NMR (C$_6$D$_6$, 298 K): δ = 0.82 (Si(C*H*$_3$)$_2$), 21.84 (Ar-*C*H$_3$), 48.66 (NCH$_2$), 118.08 (Ar-*C*H), 119.95 (Ar-*C*H), 140.01 (*m*-Ar-*C*), 153.33 (*ipso*-Ar-*C*). ^{29}Si{^{1}H} NMR (C$_6$D$_6$, 298 K): δ = –5.18 (s, *Si*Me$_2$). FTIR (Nujol, $\widetilde{\nu}/cm^{-1}$): 1585 (s), 1350 (m), 1246 (m), 1196 (s), 1070 (m), 1041 (m), 966 (m), 988 (m), 896 (s), 866 (s), 769 (s).

Synthesis of [U{tacn(SiMe$_2$NC$_6$H$_3$Me-3,5)$_3$}] (**4-U**): THF (20 mL) was added to a pre-cooled (−78 °C) mixture of [U(I)$_3$(THF)$_4$] (0.45 g, 0.5 mmol) and **2-K$_3$** (0.46 g, 0.5 mmol). The dark red reaction mixture was allowed to warm to room temperature and stirred for 16 h. Volatiles were removed under reduced pressure and the residue was extracted with toluene (2 × 10 mL) and filtered. The solution was reduced in volume to ca. 2 mL and stored at −30 °C overnight to give dark red crystals of **4-U** (0.29 g, 65%). Anal. Calcd. for $C_{36}H_{57}N_6Si_3U$: C, 48.25; H, 6.64; N, 9.38. Found: C, 47.74; H, 5.96; N, 9.53. μ_{eff} = 2.61 μ_B (Evans method). ^{1}H NMR (C$_6$D$_6$, 298 K): δ = −30.84 (br, $\nu\frac{1}{2}$ ~ 60 Hz, 6H, NC*H*$_2$), −9.53 (br, $\nu\frac{1}{2}$ ~ 60 Hz, 6H, NC*H*$_2$), –3.64 (br, $\nu\frac{1}{2}$ ~ 20 Hz, 18H, Ar-C*H*$_3$), −0.75 (br, $\nu\frac{1}{2}$ ~ 40 Hz, 6H, *o*-Ar-*H*), 0.51 (s, 3H, *p*-Ar-*H*), 8.09 (br, $\nu\frac{1}{2}$ ~ 40 Hz, 18H, Si(C*H*$_3$)$_2$). ^{13}C{^{1}H} NMR (C$_6$D$_6$, 298 K): not observed. ^{29}Si{^{1}H} NMR (C$_6$D$_6$, 298 K): δ = −270.90 (*Si*Me$_2$). FTIR (Nujol, $\widetilde{\nu}/cm^{-1}$): 1584 (s), 1344 (s), 1289 (w), 1069 (m), 1038 (m), 989 (w), 966 (m), 912 (m), 897 (s), 866 (s), 772 (s), 673 (m).

Synthesis of [U{tacn(SiMe$_2$NC$_6$H$_3$Me-4)$_3$}(Cl)] (**6**): *Method 1:* THF (20 mL) was added to a pre-cooled (−78 °C) mixture of UCl$_4$ (0.38 g, 1 mmol) and **1-K$_3$** (0.88 g, 1 mmol). The dark green reaction mixture was allowed to warm to room temperature and stirred for 16 h. Volatiles were removed *in vacuo* and the residue was extracted with THF (2 × 30 mL) and filtered. The solution was reduced in volume to ca. 2 mL and stored at −30 °C overnight to give green crystals of **6·THF** (0.16 g, 16%). *Method 2:* An excess of ^{t}BuCl (0.023 g, 0.25 mmol) was added to a pre-cooled (−10 °C) solution of **3-U** (0.050 g, 0.056 mmol) in toluene. Upon warming to room temperature, a color change to green was observed. Volatiles were removed under reduced pressure to yield **6** in quantitative crude yield as a green solid. Anal. Calcd. for $C_{33}H_{51}ClN_6Si_3U$: C, 44.56; H, 5.78; N, 9.45. Found: C, 44.56; H, 5.73; N, 9.33. μ_{eff} = 2.76 μ_B (Evans method). ^{1}H NMR (C$_4$D$_8$O, 298 K): δ = −46.31 (br, $\nu\frac{1}{2}$ ~ 70 Hz,

6H, Ar-C*H*), −15.17 (br, $\nu\frac{1}{2}$ ~ 1,200 Hz, 6H, NCH_2), 5.86 (br, $\nu\frac{1}{2}$ ~ 100 Hz, 9H, Ar-CH_3), 12.34 (br, $\nu\frac{1}{2}$ ~ 150 Hz, 6H, Ar-C*H*), 16.08 (br, $\nu\frac{1}{2}$ ~ 600 Hz, 18H, Si(CH_3)$_2$), 23.82 (br, $\nu\frac{1}{2}$ ~ 1,000 Hz, 6H, NCH_2). ^{13}C{^{1}H} and ^{29}Si{^{1}H} NMR (C_4D_8O, 298 K): not observed. FTIR (Nujol, $\widetilde{\nu}$/cm^{-1}): 1605 (s), 1501 (m), 1247 (m), 1176 (w), 1109 (w), 1085 (m), 1045 (s), 1013 (s), 945 (m), 921 (m), 905 (m), 831 (s), 776 (m), 730 (s), 708 (m).

Synthesis of [U{tacn(SiMe$_2$NC$_6$H$_3$Me$_2$-3,5)$_3$}(Cl)] (**7**): *Method 1:* THF (20 mL) was added to a pre-cooled (−78 °C) mixture of UCl_4 (0.38 g, 0.5 mmol) and **2-K$_3$** (0.92 g, 1 mmol). The dark green reaction mixture was allowed to warm to room temperature and stirred for 16 h. Volatiles were removed in vacuo and the residue was extracted with DME (2 × 20 mL) and filtered. The solution was reduced in volume to ca. 2 mL and stored at −30 °C overnight to give green crystals of **7** (0.09 g, 10%). *Method 2:* An excess of ^{t}BuCl (0.079 g, 0.85 mmol) was added to a pre-cooled (−10 °C) solution of **4-U** (0.150 g, 0.16 mmol) in toluene. Upon warming to room temperature, a color change to green was observed. Volatiles were removed under reduced pressure and the green solid was dissolved in DME (1 mL) and stored −30 °C for 8 h to give green needles of **7** (0.063 g, 42%). Anal. Calcd. for $C_{36}ClH_{57}N_6Si_3U$: C, 46.41; H, 6.17; N, 9.02. Found: C, 46.34; H, 6.30; N, 8.93. μ_{eff} = 3.20 μ_B (Evans method). ^{1}H NMR (C_6D_6, 298 K): δ = −50.42 (br, $\nu\frac{1}{2}$ ~ 200 Hz, 2H, Ar-C*H*), 1.15 (br, $\nu\frac{1}{2}$ ~ 300 Hz, 18H, Si(CH_3)$_2$), 12.67 (br, $\nu\frac{1}{2}$ ~ 1,000 Hz, 12H, NCH_2), most Ar-C*H* and Ar-CH_3 not observed. ^{13}C{^{1}H} and ^{29}Si{^{1}H} NMR (C_6D_6, 298 K): not observed. FTIR (Nujol, $\widetilde{\nu}$/cm^{-1}): 1587 (s), 1317 (s), 1184 (s), 1042 (m), 962 (w), 920 (m), 903 (m), 889 (m), 679 (m).

Supplementary Materials: The following are available online at https://www.mdpi.com/article/10.3390/inorganics9120086/s1. Figures S1–S4: structures of **3-La·0.5C$_7$H$_8$**, **4-La** and **5**, together with a space-filling diagrams of **3-U**, **4-U** and [U{tacn(SiMe$_2$NPh)$_3$}]. Tables S1 and S2: supplementary crystallographic data for all complexes. Figures S5–S9: solid state magnetic data for **3-U** and **4-U**. Figures S10–S12: EPR spectra for **3-U** and **4-U**. Figures S13–S42: NMR spectra for all complexes. CIF and checkCIF output files for the solid state structures of **3-La·0.5C$_7$H$_8$**, **3-U·0.5C$_7$H$_8$**, **4-La**, **4-U**, **5**, **6·THF** and **7**.

Author Contributions: Conceptualization, A.F., L.S.N. and D.P.M.; methodology, A.F. and D.P.M.; validation, A.F. and D.P.M.; formal analysis, all authors; investigation, A.F., F.O., I.J.V.-Y. and F.T.; data curation, A.F. and D.P.M.; writing—original draft preparation, A.F. and D.P.M.; writing—review and editing, all authors; visualization, A.F., F.T. and D.P.M.; supervision, L.S.N. and D.P.M.; project administration, A.F., D.P.M. and L.S.N.; funding acquisition, A.F., E.J.L.M., D.P.M. and L.S.N. All authors have read and agreed to the published version of the manuscript.

Funding: This research was funded by the University of Manchester and the UK Engineering and Physical Sciences Research Council (EPSRC), grant numbers EP/G037140/1 (Nuclear FiRST DTC), EP/L014416/1 and EP/K039547/1; the EPSRC UK National Electron Paramagnetic Resonance Service provided access to the EPR Facility and the SQUID magnetometer (grant number EP/S033181/1).

Data Availability Statement: The data presented in this study are openly available in FigShare at doi:10.6084/m9.figshare.16680670 and the Cambridge Structural Database, deposition numbers CCDC 1833228-1833234.

Acknowledgments: We would like to thank Ian Fallis and Thomas Tatchell from Cardiff University for helpful advice on the synthesis of tacn.

Conflicts of Interest: The authors declare no conflict of interest.

References

1. Mills, D.P.; Liddle, S.T. Ligand Design in Modern Lanthanide Chemistry. In *Ligand Design in Metal Chemistry: Reactivity and Catalysis*; Lundgren, R., Stradiotto, M., Eds.; John Wiley & Sons, Ltd.: Chichester, UK, 2016; pp. 330–363. [CrossRef]
2. Cotton, S. *Lanthanide and Actinide Chemistry*; John Wiley & Sons, Ltd.: Chichester, UK, 2006. [CrossRef]
3. Ephritikhine, M. The vitality of uranium molecular chemistry at the dawn of the XXIst century. *Dalton Trans.* **2006**, 2501–2516. [CrossRef] [PubMed]
4. Bart, S.C.; Meyer, K. Highlights in Uranium Coordination Chemistry. *Struct. Bond.* **2008**, *127*, 119–176. [CrossRef]
5. Meyer, K.; Bart, S.C. Tripodal carbene and aryloxide ligands for small-molecule activation at electron-rich uranium and transition metal centers. *Adv. Inorg. Chem.* **2008**, *60*, 1–30. [CrossRef]

6. Liddle, S.T. The Renaissance of Non-Aqueous Uranium Chemistry. *Angew. Chem. Int. Ed.* **2015**, *54*, 8604–8641. [CrossRef]
7. Gardner, B.M.; Liddle, S.T. Uranium Triamidoamine Chemistry. *Chem. Commun.* **2015**, *51*, 10589–10607. [CrossRef]
8. Maria, L.; Santos, I.C.; Sousa, V.R.; Marçalo, J. Uranium(III) Redox Chemistry Assisted by a Hemilabile Bis(phenolate) Cyclam Ligand: Uranium–Nitrogen Multiple Bond Formation Comprising a trans-$\{RN=U(VI)=NR\}^{2+}$ Complex. *Inorg. Chem.* **2015**, *54*, 9115–9126. [CrossRef]
9. Maria, L.; Bandeira, N.A.G.; Santos, I.C.; Marçalo, J.; Gibson, J.K. CO_2 conversion to phenyl isocyanates by uranium(vi) bis(imido) complexes. *Chem. Commun.* **2020**, *56*, 431–434. [CrossRef]
10. Xin, T.; Wang, X.; Yang, K.; Liang, J.; Huang, W. Rare Earth Metal Complexes Supported by a Tripodal Tris(amido) Ligand System Featuring an Arene Anchor. *Inorg. Chem.* **2021**, *60*, 15321–15329. [CrossRef]
11. Halter, D.P.; Heinemann, F.W.; Bachman, J.; Meyer, K. Uranium-mediated electrocatalytic dihydrogen production from water. *Nature* **2016**, *530*, 317–321. [CrossRef]
12. Halter, D.P.; Heinemann, F.W.; Maron, L.; Meyer, K. The role of uranium–arene bonding in H_2O reduction catalysis. *Nat. Chem.* **2018**, *10*, 259–267. [CrossRef] [PubMed]
13. Halter, D.P.; Palumbo, C.T.; Ziller, J.W.; Gembicky, M.; Rheingold, A.L.; Evans, W.J.; Meyer, K. Electrocatalytic H_2O Reduction with f-Elements: Mechanistic Insight and Overpotential Tuning in a Series of Lanthanide Complexes. *J. Am. Chem. Soc.* **2018**, *140*, 2587–2594. [CrossRef] [PubMed]
14. Castro-Rodríguez, I.; Meyer, K. Carbon Dioxide Reduction and Carbon Monoxide Activation Employing a Reactive Uranium(III) Complex. *J. Am. Chem. Soc.* **2005**, *127*, 11242–11243. [CrossRef] [PubMed]
15. Castro-Rodríguez, I.; Nakai, H.; Zacharov, L.N.; Rheingold, A.L.; Meyer, K. A Linear, O-Coordinated η^1-CO_2 Bound to Uranium. *Science* **2004**, *305*, 1757–1760. [CrossRef]
16. Monteiro, B.; Roitershtein, D.; Ferreira, H.; Ascenso, J.R.; Martins, A.M.; Domingos, A.; Marques, N. Triamidotriazacyclononane Complexes of Group 3 Metals. Synthesis and Crystal Structures. *Inorg. Chem.* **2003**, *42*, 4223–4231. [CrossRef] [PubMed]
17. Antunes, M.A.; Dias, M.; Monteiro, B.; Domingos, A.; Santos, I.C.; Marques, N. Synthesis and reactivity of uranium(iv) amide complexes supported by a triamidotriazacyclononane ligand. *Dalton Trans.* **2006**, 3368–3374. [CrossRef]
18. Camp, C.; Antunes, M.A.; García, G.; Ciofini, I.; Santos, I.C.; Pécaut, J.; Almeida, M.; Marçalo, J.; Mazzanti, M. Two-electron versus one-electron reduction of chalcogens by uranium(iii): Synthesis of a terminal U(v) persulfide complex. *Chem. Sci.* **2014**, *5*, 841–850. [CrossRef]
19. Antunes, M.A.; Coutinho, J.T.; Santos, I.C.; Marçalo, J.; Almeida, M.; Baldoví, J.J.; Pereira, L.C.J.; Gaita-Ariño, A.; Coronado, E. A Mononuclear Uranium(IV) Single-Molecule Magnet with an Azobenzene Radical Ligand. *Chem. Eur. J.* **2015**, *21*, 17817–17826. [CrossRef] [PubMed]
20. Coutinho, J.T.; Perfetti, M.; Baldoví, J.J.; Antunes, M.A.; Hallmen, P.P.; Bamberger, H.; Crassee, I.; Orlita, M.; Almeida, M.; van Slageren, J.; et al. Spectroscopic Determination of the Electronic Structure of a Uranium Single-Ion Magnet. *Chem. Eur. J.* **2019**, *25*, 1758–1766. [CrossRef]
21. Dias, A.R.; Martins, A.M.; Ascenso, J.R.; Ferreria, H.; Duarte, M.T.; Henriques, R.T. Li, Ti(III), and Ti(IV) Trisamidotriazacyclononane Complexes. Syntheses, Reactivity, and Structures. *Inorg. Chem.* **2003**, *42*, 2675–2682. [CrossRef]
22. Izod, K.; Liddle, S.T.; Clegg, W. A Convenient Route to Lanthanide Triiodide THF Solvates. Crystal Structures of $LnI_3(THF)_4$ [Ln = Pr] and $LnI_3(THF)_{3.5}$ [Ln = Nd, Gd, Y]. *Inorg. Chem.* **2004**, *43*, 214–218. [CrossRef]
23. Avens, L.R.; Bott, S.G.; Clark, D.L.; Sattelberger, A.P.; Watkin, J.G.; Zwick, B.D. A Convenient Entry into Trivalent Actinide Chemistry: Synthesis and Characterization of $AnI_3(THF)_4$ and $An[N(SiMe_3)_2]_3$ (An = U, Np, Pu). *Inorg. Chem.* **1994**, *33*, 2248–2256. [CrossRef]
24. Shannon, R.D. Revised effective ionic radii and systematic studies of interatomic distances in halides and chalcogenides. *Acta Cryst. Sect. A* **1976**, *32*, 751–767. [CrossRef]
25. Patel, D.; Wooles, A.J.; Hashem, E.; Omorodion, H.; Baker, R.J.; Liddle, S.T. Comments on reactions of oxide derivatives of uranium with hexachloropropene to give UCl_4. *New J. Chem.* **2015**, *39*, 7559–7562. [CrossRef]
26. Kiplinger, J.L.; Morris, D.E.; Scott, B.L.; Burns, C.J. Convenient Synthesis, Structure, and Reactivity of $(C_5Me_5)U(CH_2C_6H_5)_3$: A Simple Strategy for the Preparation of Monopentamethylcyclopentadienyl Uranium(IV) Complexes. *Organometallics* **2002**, *21*, 5978–5982. [CrossRef]
27. Hashem, E.; Swinburne, A.N.; Schulzke, C.; Evans, R.C.; Platts, J.A.; Kerridge, A.; Natrajan, L.S.; Baker, R.J. Emission spectroscopy of uranium(IV) compounds: A combined synthetic, spectroscopic and computational study. *RSC Adv.* **2013**, *3*, 4350–4361. [CrossRef]
28. Windorff, C.J.; Evans, W.J. ^{29}Si NMR Spectra of Silicon-Containing Uranium Complexes. *Organometallics* **2014**, *33*, 3786–3791. [CrossRef]
29. Carnall, W.T. A systematic analysis of the spectra of trivalent actinide chlorides in D_{3h} site symmetry. *J. Chem. Phys.* **1992**, *96*, 8713. [CrossRef]
30. Sur, S.K. Measurement of magnetic susceptibility and magnetic moment of paramagnetic molecules in solution by high-field fourier transform NMR spectroscopy. *J. Magn. Reson.* **1989**, *82*, 169–173. [CrossRef]
31. Jones, E.R., Jr.; Hendricks, M.E.; Stone, J.A.; Karraker, D.G. Magnetic properties of the trichlorides, tribromides, and triiodides of U(III), Np(III), and Pu(III). *J. Chem. Phys.* **1974**, *60*, 2088. [CrossRef]
32. Kindra, D.R.; Evans, W.J. Magnetic Susceptibility of Uranium Complexes. *Chem. Rev.* **2014**, *114*, 8865–8882. [CrossRef]
33. Liddle, S.T.; van Slageren, J. Actinide Single Molecule Magnets. In *Lanthanides and Actinides in Molecular Magnetism*; Layfield, R.A., Murugesu, M., Eds.; Wiley-VCH: Weinheim, Germany, 2015; pp. 315–340. [CrossRef]

34. Liddle, S.T.; van Slageren, J. Improving f-element single-molecule magnets. *Chem. Soc. Rev.* **2015**, *44*, 6655–6670. [CrossRef]
35. Moro, F.; Mills, D.P.; Liddle, S.T.; van Slageren, J. The Inherent Single-Molecule Magnet Character of Trivalent Uranium. *Angew. Chem. Int. Ed.* **2013**, *52*, 3430–3433. [CrossRef]
36. Goodwin, C.A.P.; Tuna, F.; McInnes, E.J.L.; Liddle, S.T.; McMaster, J.; Vitorica-Yrezabal, I.J.; Mills, D.P. [U^{III}{$N(SiMe_2tBu)_2$}$_3$]: A Structurally Authenticated Trigonal Planar Actinide Complex. *Chem. Eur. J.* **2014**, *20*, 14579–14582. [CrossRef] [PubMed]
37. *CrysAlisPRO*; Agilent Technologies UK Ltd.: Yarnton, UK, 2010.
38. Sheldrick, G.M. A short history of *SHELX*. *Acta Cryst.* **2008**, *A64*, 112–122. [CrossRef] [PubMed]
39. Sheldrick, G.M. Crystal structure refinement with *SHELXL*. *Acta Cryst.* **2015**, *C71*, 3–8. [CrossRef]
40. Dolomanov, O.V.; Bourhis, L.J.; Gildea, R.J.; Howard, J.A.K.; Puschmann, H. *OLEX2*: A complete structure solution, refinement and analysis program. *J. Appl. Cryst.* **2009**, *42*, 339–341. [CrossRef]
41. Farrugia, L.J. *WinGX* and *ORTEP* for Windows: An update. *J. Appl. Cryst.* **2012**, *45*, 849–854. [CrossRef]
42. *POV-Ray*; Persistence of Vision Raytracer Pty., Ltd.: Williamstown, Australia, 2004.